WHITE **PAPER** \\ **Dr. Amir Sharghi, Dr. Frank Münchow, Arun Boddu, Dr. Thomas Limmer**

Instrument Systems
KONICA MINOLTA Group

VCSEL Array Characterization: One-shot and Single-emitter-resolved Polarization and LIV+λ Measurement

In the assessment of the electro-optical characteristics of laser diodes, a variety of measurements are typically conducted, including LIV+λ characterization (together with spectrum analysis). LIV curves play a vital role in evaluating the electrical and optical performance of laser diodes. These curves are instrumental in measuring power conversion efficiency, threshold current, slope efficiency, kinks and other critical parameters. While the widespread use of LIV curves is crucial for early detection of failed laser diodes in the manufacturing process, applying these measurements to VCSEL arrays with existing solutions proves to be a challenging task. This is because VCSEL arrays often consist of numerous single emitters, ranging from a few to several hundred within the array. Consequently, performing these measurements becomes impractical and time-consuming.

This white paper addresses this challenge by extending LIV+λ measurements to individual emitters within a VCSEL array, thereby incorporating polarization measurements. The experimental design features a camera-based radiant power and polarization measurement system, coupled with an array spectroradiometer. This system provides absolute optical power measurements that are traceable to standards. Further, to assess the characteristics of the VCSEL array in diverse environmental conditions, measurements were conducted at multiple temperatures. The flexibility of the design allows for the customization of valid parameter ranges for each emitter, based on the intended application of the VCSEL. Non-functional emitters were identified during the characterization process. This design offers a rapid and comprehensive one-shot characterization of VCSEL array emitters, enabling parallelization of measurements in order to reduce overall measurement time and detect damaged or out-of-spec VCSELs at an early stage in the manufacturing process.

WHITE
PAPER

\\ 1. INTRODUCTION

VCSELs have found their way into diverse applications, steadily gaining traction as they edge out LEDs in various fields. Their market trajectory showcases significant growth, with a projected continuous upward trend. The broad applicability of VCSELs in consumer electronics stems from their unique capabilities, such as scaling optical power and emission patterns through 2D arrays of emitters. These advancements have revolutionized their use in 3D sensing and imaging.

Recently, polarized VCSELs constitute a groundbreaking innovation in laser technology, offering controlled emission of polarized light. These lasers possess intrinsic capabilities to emit light with a specific polarization orientation, a feature of immense significance across various applications. By harnessing and manipulating the polarization of emitted light, polarized VCSELs pave the way for enhanced precision in sensing.

This paper introduces a novel one-shot measurement approach, facilitating rapid and comprehensive characterization of all emitters within VCSEL arrays. Considering the continuous evolution of VCSELs, the measurement of spectrum and polarization properties for each emitter has emerged as a critical necessity. To address this, our study extends the LIV characterization of individual emitters to encompass additional properties such as spectrum and polarization, providing a more thorough understanding of VCSEL array behavior.

\\ 2. MEASUREMENT SETUP

The measurement setup consisted of a camera-based system designed for both radiant power (near-field VTC 4000) and spectrum (CAS 120-HR) measurements. These instruments were mounted on a 3D-axis translation stage, enabling precise spatial control during the measurement processes. A 12-megapixel CMOS camera was complemented by a microscopic objective that covered a field of view of 1.4 mm x 1.0 mm and 0.26 NA, and calibrated at 940nm for absolute power measurement that is traceable to national standards. Remarkably, the camera is not solely dedicated to power measurement; it possesses the unique ability to discern the polarization of each individual emitter. Simultaneously, the high-resolution array spectroradiometer (CAS 120-HR) integrated into this setup offers a spectral resolution range from 0.12 nm to 0.4 nm. Covering a spectrum from 80 nm to 160 nm, this spectroradiometer – intricately linked via fiber to the camera system – facilitates simultaneous spectrum measurements. The VCSEL array, constructed from GaAs, featured a robust configuration housing 281 emitters operating at 940 nm, delivering an optical power output of 2 W with 3 A maximum forward current with 100 % DC at 25 °C. In our measurement set up, the array was mounted on a PCB on top of an Arroyo temperature controller.

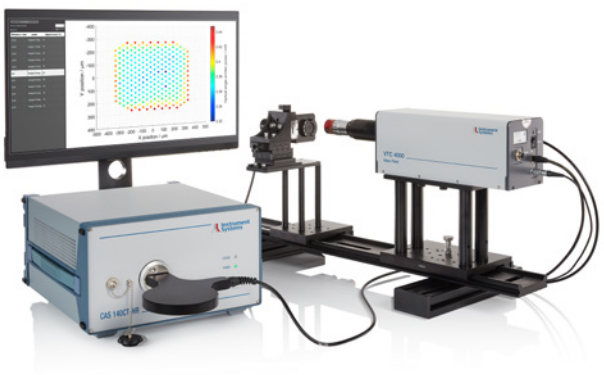

Figure 1: VTC 4000 one-shot single-emitter analysis system.

\\ 3. LIV CHARACTERIZATION OF THE WHOLE ARRAY

Leveraging a near-field system, we conducted L-I-V characterizations of the whole VCSEL array at three temperatures (25 °C, 35 °C and 40 °C), depicted in red, green and blue (Figure 2). It is evident that the threshold current for the VCSEL array is roughly around 0.21 A across all three temperature conditions. Notably, the optical power demonstrates a consistent linear increase at intermediate current levels. This trend persists due to the effective active cooling mechanisms in place, preventing the system from reaching the projected rollover point within our specified current limits.

Interestingly, the VCSEL shows an improvement in slope efficiency at lower temperatures, while maintaining the threshold current. Examining the I-V curve, the anticipated linear increase in voltage with respect to the current is observed consistently across all temperature settings.

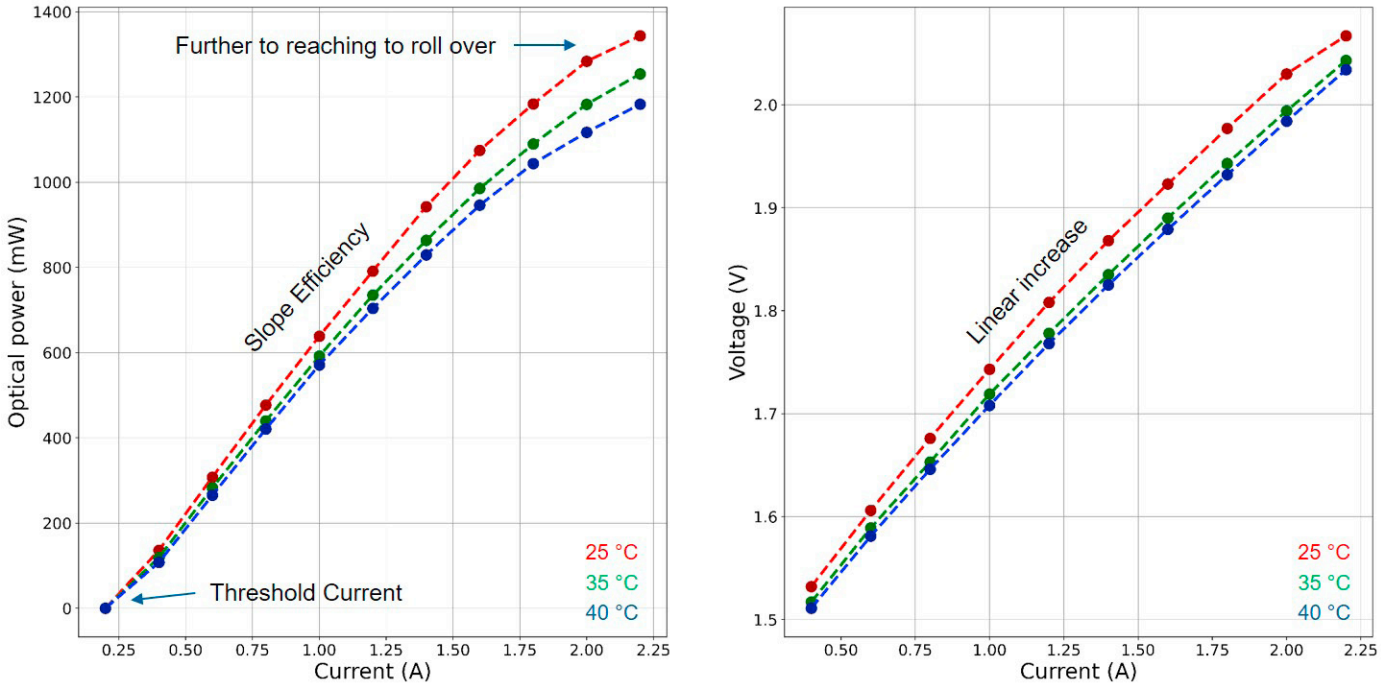

Figure 2: This figure displays the LIV characterization of the VCSEL array across varied temperatures: 25 °C (red), 35 °C (green) and 40 °C (blue). The VCSEL array was subjected to currents ranging up to 2.2 A in increments of 0.2 A. Notably, the threshold current and the slope efficiency are key parameters outlined within this characterization.

\\ 4. LIV CHARACTERIZATION OF EACH SINGLE EMITTER ACROSS THE ARRAY

Simultaneously, our capabilities extend to computing the slope efficiency and threshold current for every individual emitter within the array (Figure 3). This comprehensive depiction enables a granular understanding of how these critical parameters fluctuate spatially within the array. Here, we make a cross-temperature examination, delineating the slope efficiency and threshold current contrasts among distinct thermal conditions 25 °C, 35 °C and 40 °C, color-coded respectively in red, green and blue.

Across all emitters we observe a pattern similar to the LIV of the whole array. Individual emitters show the same threshold current at different temperatures and the slope efficiency decreases at a higher temperature. For instance, emitter 26 – indicated by arrows in Figure 3 – consistently exhibits a higher threshold current and lower slope efficiency across all temperature ranges. By excluding this defect emitter from the analysis, the refined visualizations in Figure 3B and 3E reveal a more detailed narrative of parameter variations throughout the array.

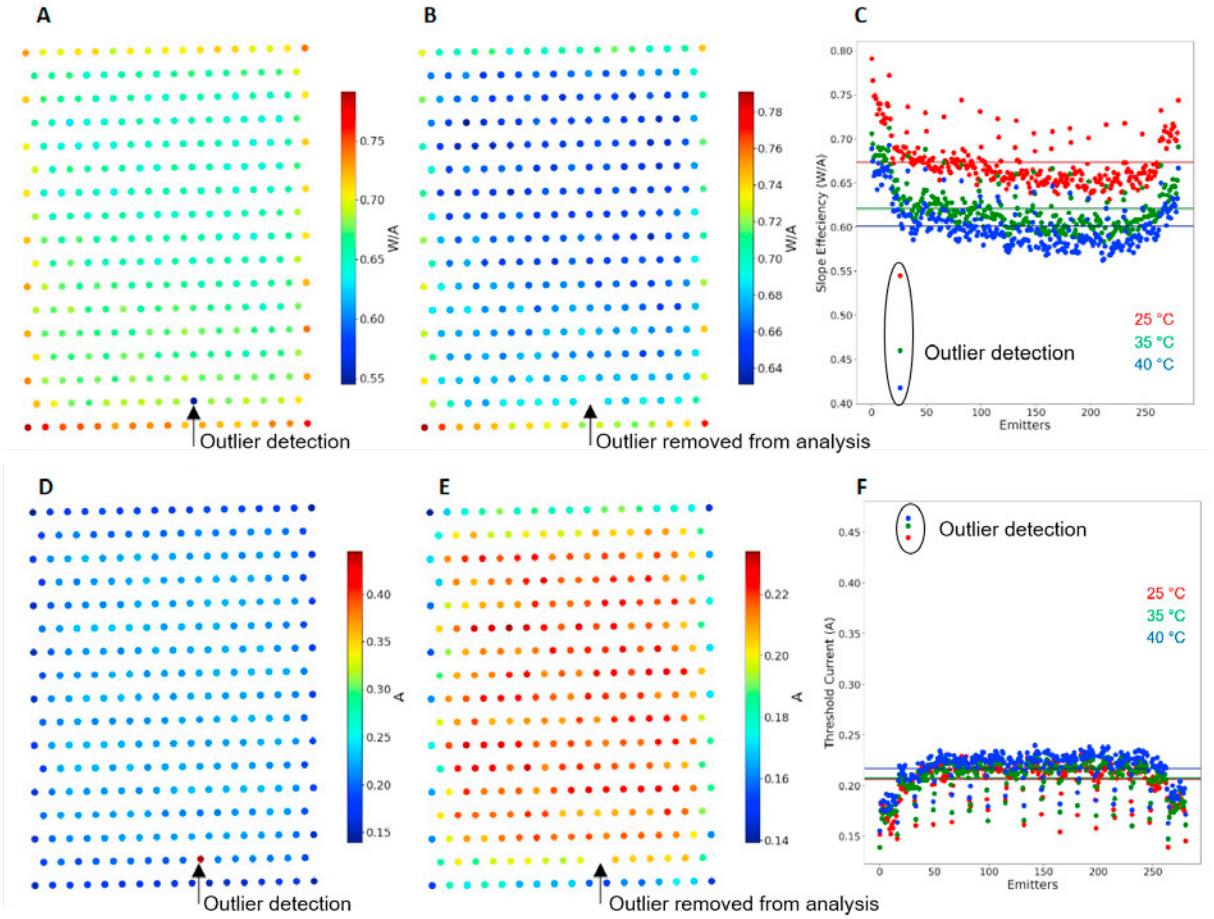

Figure 3: This figure presents the calculated slope efficiency (A-C) and threshold current (D-F) for each emitter within the VCSEL array. A depicts the slope efficiency of individual emitters at 25 °C, highlighting Emitter 26 as an outlier with significantly lower values compared to others. In plot B, Emitter 26 is omitted from the analysis for a refined view. Plot C illustrates the slope efficiency analysis across all three temperatures (25 °C, 35 °C and 40 °C, depicted in red, green and blue respectively), revealing a trend of higher slope efficiency among most emitters at 25 °C. Moving to threshold current analysis, plots D and E depict the threshold current of each emitter at 25 °C, where Emitter 26 once again appears as an outlier and is excluded in plot E for a more detailed examination. Plot F extends the threshold current analysis across all emitters and temperatures, providing a comprehensive overview of this parameter's behavior in varied thermal conditions.

\\ 5. OPTICAL BEAM CHARACTERIZATION

Additionally, the assessment encompassed four crucial parameters – optical power, numerical aperture, beam waist and beam quality M^2 – across each of the 281 emitters within the VCSEL (Figure 4). Spanning three temperature settings, the VCSEL underwent varying electrical current increments, ranging from 400 mA to 2.2 A in steps of 200 mA, to capture these measurements. While there were observable increasesin both numerical aperture (NA) and beam quality (M^2) at higher currents, no discernible changes were evident in the beam waist. Intriguingly, these parameters exhibited no distinct or definable pattern concerning temperature variations. Although numerical aperture tended towards larger values at lower temperatures, these changes were not significantly pronounced or consistent across the spectrum of temperatures studied.

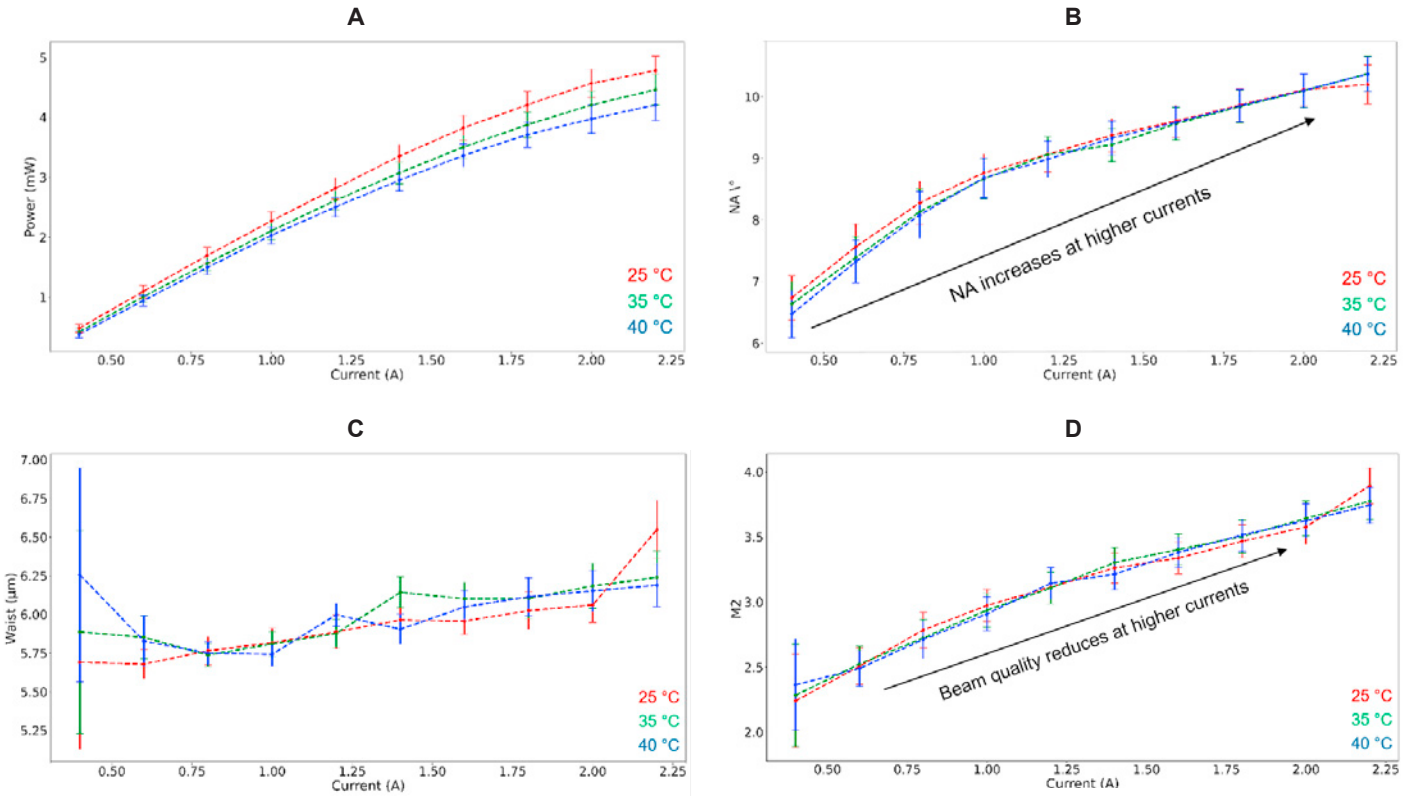

Figure 4: This figure portrays the analysis of optical power, numerical aperture (NA), beam waist and beam quality (M^2) across the emitters of the VCSEL array at three distinct temperatures (25 °C, 35 °C and 40 °C, represented by red, green and blue respectively). Surprisingly, no substantial impact of temperature variation on these parameters is discernible. However, noteworthy trends emerge: both numerical aperture (NA) and beam quality (M^2) exhibit a discernible increase with rising current levels. Conversely, the beam waist demonstrates minimal fluctuation, despite changes in current, showcasing a relatively stable behavior across varying electrical currents.

\\ 6. SPECTROMETER MEASUREMENT

Spectrometer analysis played a pivotal role in our comprehensive characterization. Specifically, we selected 15 emitters distributed across the array to undergo spectrum analysis, strategically chosen from diverse locations within the array. Similar to other measurements conducted in this study, these 15 emitters were subjected to spectrum analysis at various current levels. Figure 5 visually represents the spectra obtained from all emitters at 25 °C and across different currents, emitters at 400 mA depicted in blue, while those at 2.2 A are shown in red. An apparent forward shift in wavelength is noticeable with higher currents. Notably, at lower currents, the emitters exhibited a single mode within their spectra. However, as the current was incrementally increased, additional spectral modes emerged progressively until reaching the highest current levels.

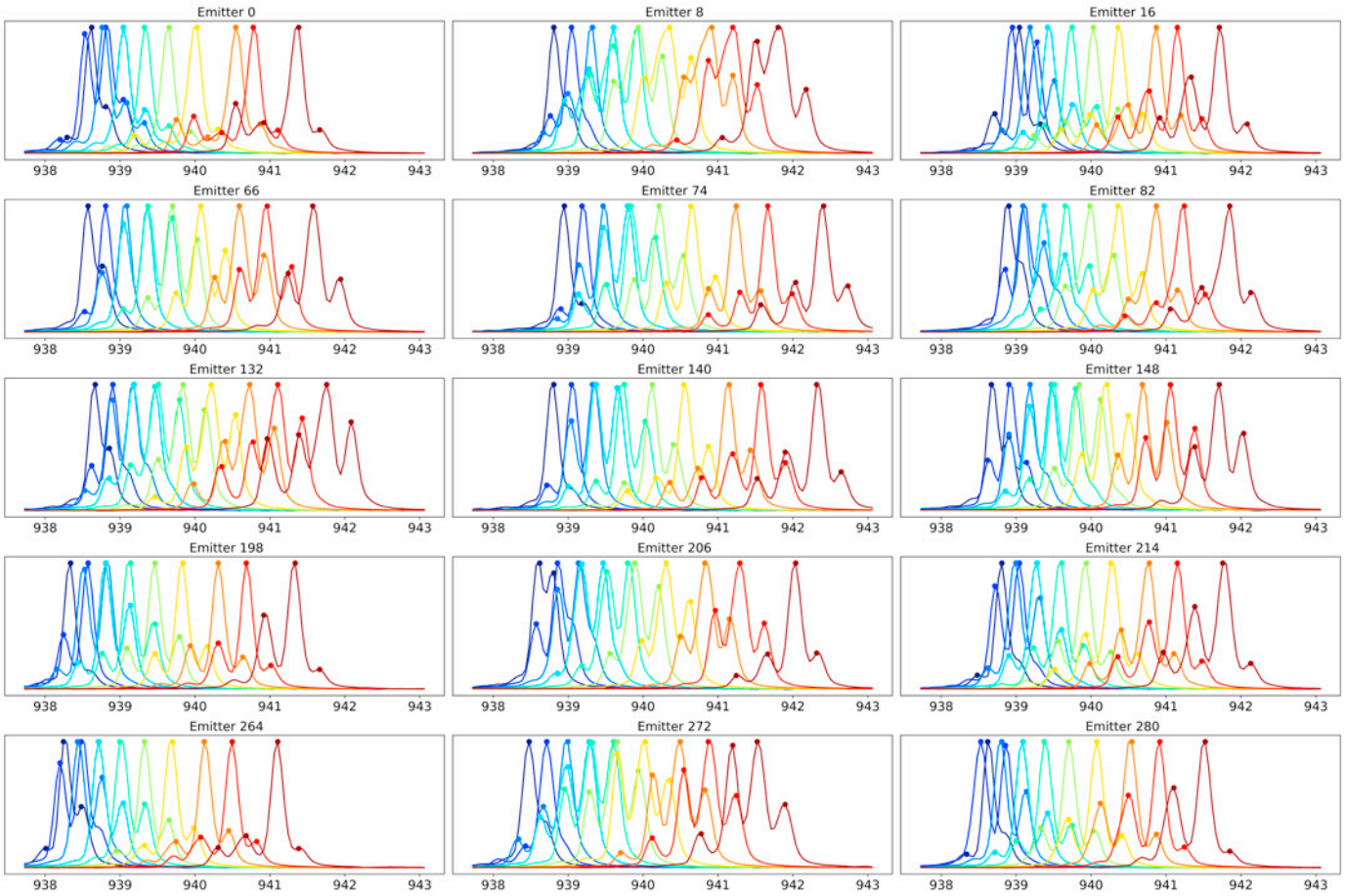

Figure 5: This figure depicts individual subplots, showcasing the spectra of emitters at 25 °C and at various currents, denoted by color gradations from blue (400 mA) to red (2.2 A). Notably, a discernible shift in the spectra at higher currents is evident, accompanied by the emergence of higher-order modes as the current levels increase. This observation underscores the dynamic changes occurring within the spectral profiles in response to incremental changes in current, shedding light on the evolution of spectral characteristics as the driving current intensifies.

Expanding our analysis, we conducted a comprehensive spectrum analysis of the VCSEL array across all three temperatures (25 °C, 35 °C and 40 °C). The outcomes of this investigation are visually depicted in Figure 6, which showcases the spectra of all 15 emitters across diverse currents including temperatures. Notably, this visualization employs color coding exclusively for temperature representation: red corresponds to 25 °C, green to 35 °C and blue to 40 °C.

One striking observation is the discernible red shift observed at higher temperatures within the emitted spectra. This red shift phenomenon becomes increasingly pronounced as the temperature elevates. This observation underscores the notable impact of temperature fluctuations on the spectral characteristics of the emitters, suggesting a clear correlation between temperature variations and the spectral shifts observed within the VCSEL array.

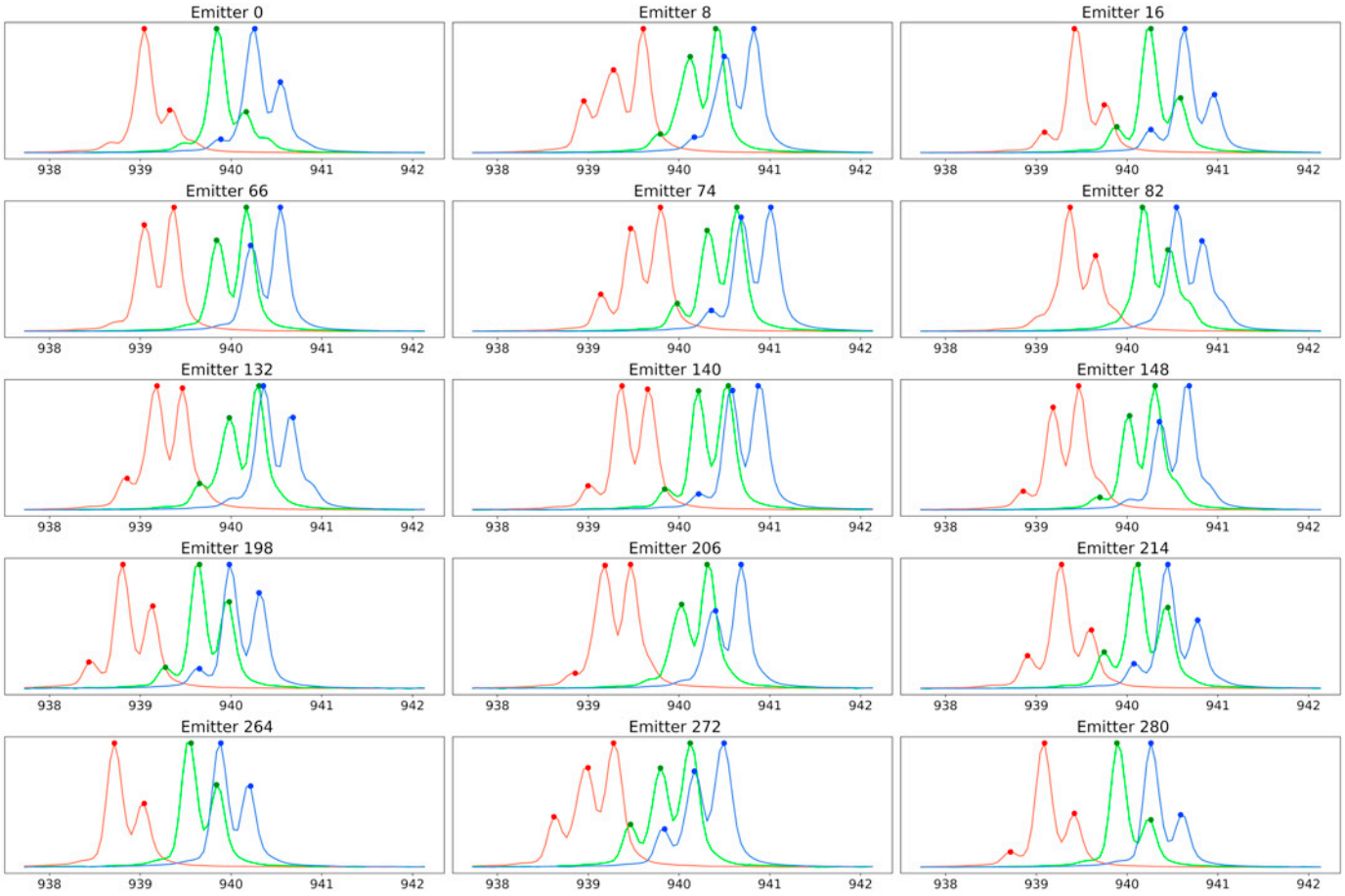

Figure 6: This figure showcases the spectra of all 15 emitters at 1.0 A and across diverse temperatures. It is worth noting that this visualization employs color coding exclusively for temperature representation: red corresponds to 25 °C, green to 35 °C and blue to 40 °C.

\\ 7. POLARIZATION MEASUREMENT

The polarization of individual emitters emerged as another fascinating parameter within our measurement scope. Within the realm of VCSELs, polarized stable emissions hold immense significance for targeted applications where specific polarizations are crucial. What sets our approach apart is the integration of polarization measurements within a single-shot solution. This innovative methodology eliminates the need for any mechanical movement in our optical design, allowing polarization measurements to be seamlessly captured alongside other crucial parameters. Figure 7 serves as an illustrative example, depicting the angle of polarization alongside the degree of polarization for a single emitter. The angle of polarization refers to the orientation of the electric field oscillation within the emitted light, often measured with respect to a reference axis and typically expressed in degrees. On the other hand, the degree of polarization quantifies the extent to which the light is polarized along a particular axis. It is a measure of purity of the light in terms of polarization, indicating the strength of the alignment of oscillations in the electromagnetic field along a specific direction. The degree of polarization is represented as a value between 0 (completely unpolarized light) and 1 (fully polarized light).

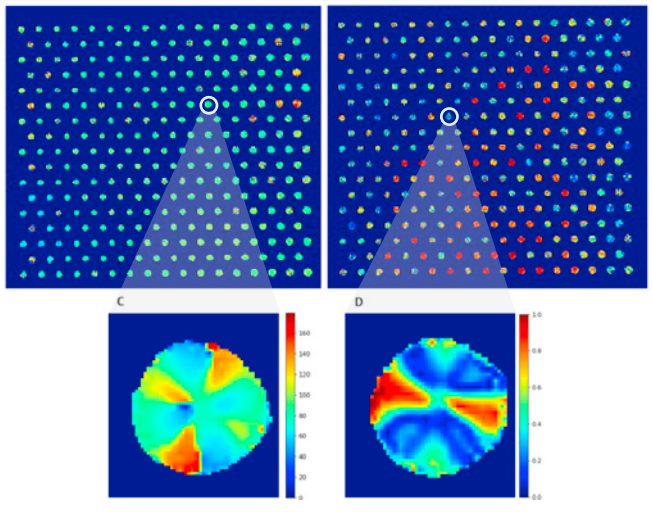

Figure 7: An illustrative example, depicting the angle of polarization alongside the degree of polarization for the whole array in A and B, as well as for a single emitter in C and D.

Our DUT in this work was not meant to have stable polarization. This can also be observed in our measurements results. Some emitters seem to be partially polarized, but in general we observe that our VCSEL array is randomly polarized.

Further, we derived the light-current (L-I) curves for two distinct polarization orientations: 0 degrees and 90 degrees. This comprehensive approach allows us to examine and compare the characteristics of the emitted light in terms of different polarizations (Figure 8A and 8B). Moreover, alongside the L-I curves, we calculated the polarization extension ratio (PER). This metric serves as a vital indicator quantifying the disparity in emitted power between the two orthogonal polarization states. By measuring and evaluating the PER, we gain valuable insights into the polarization properties of VCSELs (Figure 8C). This analysis facilitates a thorough understanding of how VCSELs behave under differing polarization orientations, shedding light on their polarization-dependent performance and helping to optimize their functionality for targeted applications. At the same time, these comprehensive calculations and analyses were extended across our three distinct temperature conditions. Throughout these evaluations, the color representation remained consistent: red denoting 25 °C, green representing 35 °C and blue indicating 40 °C.

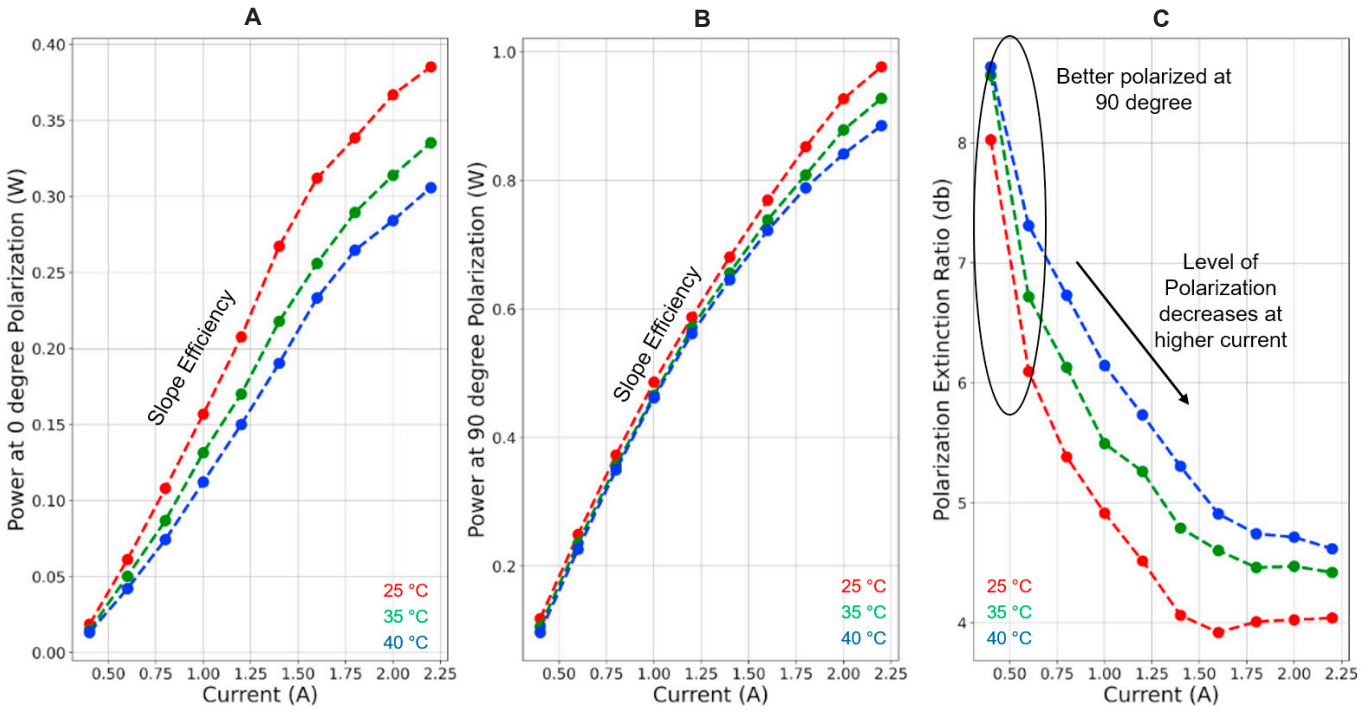

Figure 8: L-I curve for 0- and 90-degree polarization together with the polarization extension ration (PER). Red corresponds to 25 °C, green to 35 °C and blue to 40 °C

The L-I curve for 90-degree polarization exhibited a more pronounced increase in response to current increments. Additionally, the region where power linearly increased with current spanned a larger area within the 90-degree polarization curve. At lower temperatures, we observed a heightened slope efficiency within the L-I curve for both polarization orientation. This finding signifies an enhanced power output per unit of current, highlighting the potential efficiency gains at lower temperatures. A pivotal observation lies in the total power output between the two polarization orientations. Notably, the L-I curve for 90-degree polarization consistently showcases significantly higher total power compared to the 0-degree polarization L-I curve.

This comprehensive analysis examines the nuanced behaviors of VCSELs under varying polarization orientations and temperatures, revealing key performance disparities crucial for optimizing their functionality in diverse applications. PER is expressed in logarithmic form due to the nature of polarization measurements that often involve comparing powers that span a wide range of values. A higher PER indicates a greater disparity in power between the orthogonal polarization states, reflecting the efficiency or purity of the polarized light (Figure 8C). We can also conclude from Figure 8C that at lower temperature, the VCSEL array is better polarized at 90 degrees.

\\ 8. CONCLUSION

Our study encompassed a comprehensive assessment, conducting LIV characterization for the entire array, as well as for each individual emitter. We meticulously analyzed various optical characteristics of all emitters, parameters such as optical power, beam waist, numerical aperture (NA) and M^2. Expanding our investigation, we conducted spectrum measurements for 15 randomly selected emitters across the array, along with polarization assessments for all individual emitter. To comprehend the effects of temperatures on the operation of the VCSEL array, we executed these assessments across three distinct temperature settings. The distinctive single-shot capacity of our methodology enabled efficient measurement of these parameters for every emitter, establishing our approach as swift and reliable, offering a sturdy foundation for thorough analysis. We believe that such thorough and detailed characterization of individual emitters holds immense significance, particularly in high-demand applications such as facial recognition, 3D sensing, in-cabin sensing, LiDAR and ranging.

Our emphasis on polarization measurements for each emitter underscores their criticality. The necessity for a meticulous delineation of requirements to establish specific criteria for acceptable measurement variations becomes evident. Defining these criteria, aligned with the measurement procedure tailored to the DUT and its intended usage, enables swift identification of underperforming or out-of-specification emitters. This empowers manufacturers to guarantee product compliance without incurring additional packaging costs, thereby optimizing the manufacturing process.

Instrument Systems GmbH | Kastenbauerstr. 2 | 81677 Munich, Germany | ph: +49 (0)89 45 49 43-58
fax: +49 (0)89 45 49 43-11 | info@instrumentsystems.com | www.instrumentsystems.com